**Atmospheric
Chemistry
and Physics
Discussions**

On the volatility and production mechanisms of newly formed nitrate and water soluble organic aerosol in Mexico City

C. J. Hennigan[1], A. P. Sullivan[2,*], C. I. Fountoukis[3], A. Nenes[2,3], A. Hecobian[2],
O. Vargas[2], A. T. Case Hanks[2], L. G. Huey[2], B. L. Lefer[4], A. G. Russell[1], and
R. J. Weber[2]

[1]School of Civil and Environmental Engineering, Georgia Institute of Technology, Atlanta, GA, 30332-0340, USA
[2]School of Earth and Atmospheric Sciences, Georgia Institute of Technology, Atlanta, GA, 30332-0340, USA
[3]School of Chemical and Biomolecular Engineering, Georgia Institute of Technology, Atlanta, GA, 30332-0340, USA
[4]Geosciences Department, University of Houston, Houston, TX, 77204-5007, USA
[*]now at: Colorado State University, Ft. Collins, CO, USA

Correspondence to: C. J. Hennigan (chennigan@eas.gatech.edu)

Title Page

Abstract | Introduction

Conclusions | References

Tables | Figures

◀ | ▶

◀ | ▶

Back | Close

Full Screen / Esc

Printer-friendly Version

Interactive Discussion

Abstract

Measurements of atmospheric gases and fine particle chemistry were made in the Mexico City Metropolitan Area (MCMA) at a site ~30 km down wind of the city center. Ammonium nitrate (NH_4NO_3) dominated the inorganic aerosol fraction and showed a distinct diurnal signature characterized by rapid morning production and a rapid mid-day concentration decrease. The concentration increase was due to both secondary formation and entrainment from the free troposphere. A majority (approximately two-thirds) of the midday concentration decrease was caused by dilution from boundary layer expansion, however a significant fraction (approximately one-third) of the nitrate loss was due to particle evaporation. The water-soluble organic carbon fraction of fine particles (WSOC) and nitrate were highly correlated (R^2=0.80) for the entire three-day analysis period, however the WSOC-nitrate correlation was highest (R^2=0.88) between the hours of 08:00–12:45, indicating similar sources and processing during this period. The results show that WSOC also experienced evaporation losses and that a significant fraction of the MCMA secondary organic aerosol (SOA) measured at the surface was semi-volatile.

1 Introduction

Secondary organic aerosol (SOA) is an important component of ambient particulate matter. It frequently comprises a large fraction of the total organic carbon aerosol (OC), often greater than 50% on a carbon mass basis (Kanakidou et al., 2005). Despite its high relative abundance and ubiquitous presence in the atmosphere, many characteristics of SOA are not well understood and require better characterization. These include chemical composition, relative contributions from anthropogenic and biogenic sources, and major formation mechanisms. These uncertainties preclude the accurate modeling of SOA concentrations (e.g. Henze and Seinfeld, 2006).

One route for SOA formation is through gas-phase oxidation of volatile organic com-

C. J. Hennigan et al.

pounds (VOCs), which leads to less volatile products that may condense into the aerosol phase. Many of the condensed species are subsequently semi-volatile (i.e. they exist in both the gas and particle phase at typical atmospheric conditions) and contribute significantly to organic aerosol mass (Seinfeld and Pankow, 2003). Though this broad conceptual framework is generally accepted, the semi-volatile nature of SOA is not well constrained.

SOA chemical composition determines its volatility. In general, low molecular weight compounds are more volatile than high molecular weight compounds (e.g. oligomers). Multiple smog chamber experiments have analyzed SOA volatility, including Offenberg et al. (2006), Kalberer et al. (2004), and An et al. (2007). These studies have provided information about the volatility of specific secondary products (i.e. the volatility of SOA from α-pinene/ozone and α-pinene/NO$_x$ experiments (An et al., 2007). Thermal properties of ambient OA and SOA have been examined by analyzing the data (thermograms) from certain organic carbon analyzers (Yu et al., 2004), but the analyses were conducted at temperature heating profiles such that elucidating information on volatility in conditions relevant to the atmosphere was not possible.

Numerous studies focused on ambient aerosol have examined a semi-volatile fraction of the bulk organic aerosol using a sampling-based operational definition (e.g. Modey and Eatough, 2004). Semi-volatile organic matter (SVOM) is defined as those compounds which penetrate a quartz filter but are collected on a backup charcoal impregnated glass fiber filter in a gas-denuded sample stream. Using this operational definition, SVOM has been found to contribute significantly to PM$_{2.5}$ mass in urban and rural locations in both winter and summer seasons (Wilson et al., 2006). Using the same operational definition, Eatough et al. (2003) coupled SVOM measurements with a source apportionment model to investigate sources and composition of aerosol in Utah. During a period in 2000 that was heavily influenced by biomass burning, they found that over 50% of SOA was semi-volatile.

Though some work has been done on the volatility of SOA, overall knowledge of ambient SOA volatility remains low. In this paper, the semi-volatile nature of SOA mea-

sured in the Mexico City Metropolitan Area (MCMA) is examined through a comparison with ammonium nitrate (NH_4NO_3), a semi-volatile species whose thermodynamic properties are well-understood.

2   Methods

Measurements of aerosol and gas-phase species were made in March 2006 as part of the Megacity Initiative: Local and Global Research Objectives (MILAGRO) field campaign. The study was focused on examining the chemical nature and processing of pollution outflow from the MCMA. Data reported here are from the ground-based measurement site, T1, located approximately 30 km downwind of the MCMA city center at the Universidad Tecnológica de Tecámac (lat 19.708, lon −98.982). All concentrations are reported at ambient temperature and pressure.

Inlets for aerosol measurements were located approximately 10 m above the ground and were fitted with cyclones (URG, Chapel Hill, NC) to select particles with aerodynamic diameters less than 2.5 μm ($PM_{2.5}$). Water-soluble organic carbon (WSOC) aerosol was measured with a particle-into-liquid sampler (PILS) coupled to a total organic carbon analyzer (Sievers, Boulder, CO) (Sullivan et al., 2004). Aerosol inorganic ionic components were measured by a PILS coupled to dual ion chromatographs (IC) (Metrohm, Herisau, Switzerland) (Orsini et al., 2003) to quantify a suite of both cations and anions. A Sunset Labs OCEC field analyzer (Sunset Laboratory Inc., Tigard, OR) following Bae et al. (2004) recorded particulate organic carbon (OC). Hydroxyl (OH) and peroxy (RO_2) radical concentrations were measured with a chemical ionization mass spectrometer (CIMS) (Sjostedt et al., 2007). Measurements of nitric oxide (NO) and photolysis rates (J values) were made with a chemiluminescence detector (Ryerson et al., 2000) and an actinic flux spectroradiometer (Shetter and Muller, 1999), respectively. Ozone (O_3) was measured with a commercial UV photometric O_3 analyzer (TECO, Model 49C). Finally, 1-min measurements of carbon monoxide (CO) were obtained with a 50% duty cycle with a commercial nondispersed infrared absorption in-

strument (Thermo Environmental Systems, Model 48C) modified according to Parrish et al. (1994).

3 Results and discussion

Measurements at T1 were performed from 7–31 March 2006, however the present analysis focuses only on the period of 27–29 March. The selected period is fairly representative of the month, but with the greatest consistency in the diurnal behavior of $PM_{2.5}$ mass and the highest daily maximum NO_3^- concentrations (Fig. 1). It was also the period least impacted by biomass burning (Stone et al., 2007), which along with SOA is a source of fine particle WSOC (Sullivan et al., 2006).

3.1 NH_4NO_3 Formation

NH_4^+ and NO_3^- were highly correlated (R^2=0.82) and dominated the inorganic $PM_{2.5}$ fraction, accounting for an average of 57% of measured inorganic mass. Concentrations of both species increased rapidly with increasing solar radiation starting at approximately 07:30 (CST, UTC−6 h) (Fig. 1), suggesting photochemical aerosol formation. The NO_3^- concentration reached its daily maximum near 11:00 of 18.1 $\mu g\,m^{-3}$, an increase of 13.8 $\mu g\,m^{-3}$ (more than 300%) over pre-sunrise concentrations. A box model was constructed to investigate the contribution of secondary nitrate formation to this AM increase on 3/27 and 3/28, the days for which boundary layer height (BL) data were available. From Seinfeld and Pandis (1998), the governing equation for an Eulerian box model with a well-mixed and expanding boundary layer is

$$\frac{dc_i}{dt} = \frac{1}{H(t)}Q_i + R_i - \frac{1}{H(t)}S_i + \frac{u}{\Delta x}(c_i^0 - c_i) + \frac{1}{H(t)}\frac{dH}{dt}(c_i^a - c_i) \tag{1}$$

where c_i is the species i concentration, c_i^0 is the species i background concentration, c_i^a is the species i concentration aloft, Q_i is the emission rate, R_i is the chemical

SOA and nitrate volatility in Mexico City

C. J. Hennigan et al.

|◄ | ►|

◄ | ►

Back | Close

Full Screen / Esc

Printer-friendly Version

Interactive Discussion

production rate, S_i is the loss rate, u is the wind speed (with constant Δx direction), and $H(t)$ is the BL height. For the purpose of modeling NO_3^- at the T1 site during the hours of 07:30–11:00, a number of assumptions were made to simplify the model. The removal rate, S_i, was neglected from the model because the dry deposition velocity for 0.1–2.5 μm particles (0.01–0.2 cm s^{-1} (Seinfeld and Pandis, 1998)) is not important on the timescale of several hours. Wind speeds, which generally ranged from 1–2 m/s during the period of interest, were too low to make advection an important process on the timescale of several hours, either. Each day before 11:00, the ISORROPIA-II thermodynamic equilibrium model (Nenes et al., 1998; Fountoukis and Nenes, 2007) predicted that greater than 90% of total nitrate (NO_3^- + HNO_3 (g)) partitioned in the particle phase due to thermodynamic conditions that favored the condensed phase, including low T, high RH, and excess ammonia gas (NH_3) (Fountoukis et al., 2007). Thus all HNO_3 (g) produced was assumed to contribute to the observed aerosol nitrate loading. The HNO_3 (g) formation rate (μg m^{-3} h^{-1}), R_i, was calculated as $k \cdot [NO_2] \cdot [OH]$, where k is the temperature-dependent kinetic rate constant (Sander et al., 2006), NO_2 was calculated from observations of NO, O_3, J values, and RO_2 assuming photochemical steady state, and OH was measured. Applying the stated assumptions gives

$$\frac{dc_i}{dt} = k \cdot [NO_2] \cdot [OH] + \frac{1}{H(t)}\frac{dH}{dt}(c_i^a - c_i) \qquad (2)$$

The model used BL depth data from Shaw et al. (2007) and NO_3^- measurements to solve for c_i^a, the NO_3^- concentration in air entrained by the expanding BL. The model results indicate that approximately 75% of the observed nitrate concentration increase was due to secondary photochemical production while approximately 25% was due to entrainment from the free troposphere. Salcedo et al. (2006) observed similar temporal behavior in the MCMA, with morning production of HNO_3 (g) immediately followed by NH_4NO_3 formation, and the trend appears to be a common phenomenon in the MCMA.

3.2 Nitrate loss

The NO_3^- peak was short lived, as concentrations began to drop precipitously at approximately 11:00 (Fig. 1). Over the period between ~11:00 and ~12:45, the NO_3^- concentration decreased by an average of $14.9\,\mu g\,m^{-3}$, an 82% drop from the peak concentration. This decrease occurred while the HNO_3 (g) production rate remained relatively high. Causes of the dramatic NO_3^- concentration decrease following the late morning maximum were likely some combination of boundary layer dilution and chemical processes (i.e. particle evaporation). Precipitation data showed that wet deposition was not important on any of the days in question. We first investigate the role of chemical processes, followed by the effects of meteorological processes on ambient concentrations.

The effect of a thermodynamic phase shift on NO_3^- was examined with ISORROPIA-II. The model uses inputs of ambient temperature, relative humidity, and total concentrations (gas + particle) of inorganic species to predict the equilibrium state of each species along with the aerosol water concentration. Model results are shown in Fig. 2. Based on rising ambient temperature and decreasing relative humidity, the model predicted a rapid phase shift of NO_3^- to HNO_3 (g). NH_4NO_3 is semi-volatile and is sensitive to changes in RH and temperature (both of which directly impact aerosol water content), with higher temperature (lower RH) favoring the gas phase and lower temperature (higher RH) favoring the particle phase. It is notable that the predicted equilibrium shift coincided with the large observed decrease in NO_3^- concentration (Fig. 2). The model predicted an average morning aerosol water concentration maximum of $15.4\,\mu g\,m^{-3}$, followed by a rapid concentration decrease to $1.2\,\mu g\,m^{-3}$ that preceded the nitrate concentration drop by approximately 1 h. Given additional time for aerosol evaporation following the water loss, the timescale of this observed delay is consistent with the analysis of Fountoukis et al. (2007). The observational data and model results agree well and suggest that, despite continued production of HNO_3 (g) and available NH_3 (g), changing ambient conditions produced a rapid shift in the equilibrium of the system

towards the gas phase and were responsible for some fraction of the observed NO_3^- concentration decrease.

Dilution must also be considered because the boundary layer underwent rapid expansion during the nitrate decrease. The box model with BL depth data from Shaw et al. (2007) was used to assess the impact of dilution on 3/27 and 3/28, the two days for which BL depth data were available. On these two days, dilution accounted for approximately 66% of the observed nitrate concentration decrease. There were two major differences between the assumptions used to generate Eq. (2) and those used for the concentration decrease analysis. Though the photochemical production of HNO_3 (g) continued while the nitrate concentration fell, this term (R_i) was excluded from the model because, unlike the morning hours, the fraction of total nitrate in the aerosol phase was not constant and was rapidly shifting to favor the gas phase. Additionally, between the hours of 11:00 and 12:45, the NO_3^- concentration aloft, c_i^a, was assumed to be zero. Both of these simplifications result in an overestimation of the dilution impact. Thus, the estimated 66% dilution loss is an upper bound and indicates that at least 34%, but likely more, of the observed nitrate loss was due to particle evaporation. Because of the observed consistency in the diurnal trends of meteorological parameters and pollutants over the three day period, it can be assumed that the losses from dilution on 3/29 were similar to those on 3/27 and 3/28. In further support of this analysis, an approximation of BL dilution on 3/29 was made using two independent chemical tracers, water vapor and carbon monoxide (CO). Assuming aloft CO and water vapor concentrations of 100 ppb and 6500 ppm, respectively, the nitrate losses from dilution and evaporation were estimated at 70% and 30%, respectively. Though there is a high amount of uncertainty in this estimate, the results on 3/29 were consistent with those obtained using the measured BL depth and suggest that the behavior on 3/29 was similar to that on 3/27 and 3/28.

3.3 Photochemical WSOC production

The PILS-WSOC method provides an approximate measurement of SOA mass (Sullivan et al., 2006; Kondo et al., 2007). Biomass burning is also a source for particulate WSOC and may account for some of the measured background WSOC observed in Mexico City, however, the biomass burning tracer acetonitrile (de Gouw et al., 2006) did not follow the diurnal WSOC trend on these selected three days and so we conclude that the consistent diurnal profile is mainly due to SOA formation.

For the three days, the WSOC concentration increased an average of 1.6 μg C m^{-3} (a 50% increase) over the three-hour period from 08:00 to 11:00 each day and had an average peak of 4.8 μg C m^{-3} before noon (Fig. 1). Similar to NO$_3^-$, the WSOC concentration experienced a daily decrease shortly after the morning maximum. Between ~11:00 and ~12:45, the WSOC concentration decreased an average of 2.7 μg C m^{-3}, a 56% decrease from the peak concentration.

Overall, WSOC and NO$_3^-$ were highly correlated (R^2=0.80), indicating similar sources and atmospheric processing. However, between the hours of 08:00–12:45, a period that included the concentration increase and decrease, the correlation was even stronger (Fig. 3). During this time the coefficient of determination (R^2) was 0.88 (all three days), 0.92 (3/27), 0.85 (3/28), and 0.98 (3/29) (Fig. 3). The high correlations show that during these periods the sources and atmospheric processes affecting both species were likely the same. Thus, similar to NO$_3^-$, it is probable that a large fraction of the WSOC concentration increase was due to secondary formation. Multiple studies have observed increased WSOC:OC ratios during periods of SOA enhancement (Sullivan et al., 2004; Kondo et al., 2007). WSOC comprised, on average, 44% of OC for the three-day period, however, the ratio increased throughout the morning and was 52%, on average, by the late-morning peak. The correlation with solar radiation and the increasing WSOC:OC ratio also provides evidence for photochemical SOA formation. Because the contributions from biomass burning were presumed to be small, it is likely that anthropogenic sources were responsible for the majority of the observed

Title Page

Abstract | Introduction

Conclusions | References

Tables | Figures

|◄ | ►|

◄ | ►

Back | Close

Full Screen / Esc

Printer-friendly Version

Interactive Discussion

HNO$_3$ (g), NO$_3^-$, and WSOC. Furthermore, the strong WSOC-NO$_3^-$ correlation is also suggestive that OH was the primary oxidation pathway in the observed SOA formation. Similar photochemical production of SOA has been observed previously in the MCMA (Salcedo et al., 2006).

3.4 NO$_3^-$ versus WSOC loss

The high correlation between WSOC and NO$_3^-$ indicates that the processes inducing the WSOC and NO$_3^-$ concentration decreases were also similar and that the volatility of WSOC was similar to that of NO$_3^-$ under the thermodynamic conditions encountered during these observations. This implies that roughly two-thirds (1.8 μg C m^{-3}) of the observed WSOC concentration decrease was due to dilution, while roughly a third (0.9 μg C m^{-3}) was due to evaporation losses. If the same reasoning is applied to both NO$_3^-$ and WSOC losses, then the estimate also represents a lower bound on the evaporation losses and indicates that at least 20% of the WSOC (at peak concentration) partitioned back to the gas phase. It is possible that most of the WSOC produced in the early morning was semi-volatile, but the rapid dilution due to boundary layer expansion limits the extent to which this process can be investigated by this approach.

These findings provide insight into the semi-volatile nature of ambient SOA, an area in which knowledge is currently limited. Specifically, fresh SOA with a large anthropogenic component in fairly non-acidic aerosol possesses similar semi-volatile properties to NH$_4$NO$_3$ at the T and RH recorded here (Fig. 1). Grieshop et al. (2007) found the partitioning of fresh biogenic SOA generated in a smog chamber to be reversible when subjected to isothermal dilution which, when combined with the present results, suggests that fresh SOA (age <4–5 h) of both biogenic and anthropogenic origin may partition back to the gas phase to maintain equilibrium. Overall, these results support the findings of Wilson et al. (2006) who found the semi-volatile character of a large fraction of the organic aerosol (primary plus secondary) to be similar to that of NH$_4$NO$_3$ in filter sampling performed in both urban and rural locations.

The results also suggest that, similar to nitrate, the loss of aerosol water did impact WSOC concentrations. A study by Loeffler et al. (2006) found that when aqueous particles containing glyoxal and methylglyoxal were evaporated, there was minimal loss of particulate organic mass due to oligomer formation. If the observed evaporation of liquid water did induce oligomer formation, then it occurred here on a small scale that did not have a substantial effect on the stabilization of semi-volatile SOA species. The present results do not provide evidence for or against significant oligomer formation, but they do suggest a minimum time delay of several hours before potential oligomer formation and overall SOA stability occurs on a large scale. When considering the question of oligomer formation, the observed aerosol acidity is also noteworthy. Studies suggest that oligomer formation is enhanced in the presence of acidic particles (Gao et al., 2004). In this case if oligomer formation did occur, it was in the presence of a fairly non-acidic aerosol, as evidenced by an abundance of available NH_3 (g) and the simultaneous presence of significant SO_4^{2-} and NO_3^- concentrations in the aerosol phase.

Finally, airborne measurements made over the sampling sites during MILAGRO have also been used to investigate the production of SOA and NO_3^- by changes in concentrations with respect to CO as plumes were advected away from the urban region (Kleinman et al., 2007). They found that NO_3^- and SOA production were not similar, as observed on the surface; SOA was still produced relative to CO when net NO_3^- production had apparently stopped. They concluded that this was due to the more semi-volatile nature of NO_3^- than SOA. These differences between the surface measurements and aloft may be due to lower temperatures and higher RH aloft, and high but different volatility dependences of SOA and NO_3^-. These types of differences show that extrapolating observations of SOA production rates recorded in one study directly to other environments may be problematic.

4 Conclusions

In 2006, gas phase and $PM_{2.5}$ aerosol measurements were made in the Mexico City Metropolitan Area as part of the MILAGRO field study. For three days (27 March–29 March), NO_3^- and WSOC were highly correlated (R^2=0.80). This correlation was even
5 stronger (R^2=0.88) during the morning and early afternoon hours when concentrations of these species grew quickly and then fell even more rapidly. The morning NO_3^- concentration increase was predominantly from secondary photochemical production. The NO_3^- concentration peaked before noon and subsequently experienced a rapid concentration decrease. Box model and aerosol equilibrium model results indicate that
10 at least one-third of the nitrate concentration decrease was due to particle evaporation while the rest was due to dilution from boundary layer expansion. Assumptions used to generate the box model make the evaporation estimate a lower bound, and indicate that the impact of evaporation was likely higher. Due to the high correlation between WSOC and NO_3^-, enhanced during the morning and early-afternoon hours, it is likely
15 that the sources and chemical processes affecting both species were similar. This means that the WSOC concentration increase, while less dramatic than that of NO_3^-, was caused predominantly from SOA formation. The source of this SOA was likely anthropogenic, with OH reaction being the initiator. Similarly, the WSOC concentration decrease was likely due partly to boundary layer dilution and partly to aerosol evapo-
20 ration, with evaporation accounting for at least one-third of the decrease. The results provide novel insight into the semi-volatile nature of fresh, anthropogenic, ground-level SOA, however their translation to other environments requires further examination.

SOA and nitrate volatility in Mexico City

C. J. Hennigan et al.

Title Page

Abstract	Introduction
Conclusions	References
Tables	Figures

|◄ | ►|

◄ | ►

Back | Close

Full Screen / Esc

Printer-friendly Version

Interactive Discussion

References

An, W. J., Pathak, R. K., Lee, B. H., and Pandis, S. N.: Aerosol volatility measurement using an improved thermodenuder: Application to secondary organic aerosol, J. Aerosol Sci., 38(3), 305–314, 2007.

5 Bae, M. S., Schauer, J. J., DeMinter, J. T., and Turner, J. R.: Hourly and daily patterns of particle-phase organic and elemental carbon concentrations in the urban atmosphere, J. Air Waste Manage. Assoc., 54(7), 823–833, 2004.

de Gouw, J. A., Warneke, C., Stohl, A., Wollny, A. G., Brock, C. A., Cooper, O. R., Holloway, J. S., Trainer, M., Fehsenfeld, F. C., Atlas, E. L., Donnelly, S. G., Stroud, V., and Lueb, A.:

10 Volatile organic compounds composition of merged and aged forest fire plumes from Alaska and western Canada, J. Geophys. Res., 111(D10), 20, doi:10.1029/2005JD006175, 2006.

Eatough, D. J., Long, R. W., Modey, W. K., and Eatough, N. L.: Semi-volatile secondary organic aerosol in urban atmospheres: meeting a measurement challenge, Atmos. Environ., 37(9–10), 1277–1292, 2003.

15 Fountoukis, C. and Nenes, A.: ISORROPIA II: A Computationally Efficient Aerosol Thermody-namic Equilibrium Model for K^+, Ca^{2+}, Mg^{2+}, NH_4^+, Na^+, SO_4^{2-}, NO_3^-, Cl^-, H_2O Aerosols, Atmos. Chem. Phys., 7, 4639–4659, 2007,
http://www.atmos-chem-phys.net/7/4639/2007/.

Fountoukis, C., Nenes, A., Sullivan, A., Weber, R., VanReken, T., Fischer, M., Matías, E., Moya,

20 M., Farmer, D., and Cohen, R. C.: Thermodynamic characterization of Mexico City aerosol during MILAGRO 2006, Atmos. Chem. Phys. Discuss., 7, 9203–9233, 2007,
http://www.atmos-chem-phys-discuss.net/7/9203/2007/.

Gao, S., Ng, N. L., Keywood, M., Varutbangkul, V., Bahreini, R., Nenes, A., He, J. W., Yoo, K. Y., Beauchamp, J. L., Hodyss, R. P., Flagan, R. C., and Seinfeld, J. H.: Particle phase

25 acidity and oligomer formation in secondary organic aerosol, Environ. Sci. Technol., 38(24), 6582–6589, 2004.

Grieshop, A. P., Donahue, N. M., and Robinson, A. L.: Is the gas-particle partitioning in alpha-pinene secondary organic aerosol reversible?, Geophys. Res. Lett., 34, L14810, doi:10.1029/2007GL029987, 2007.

30 Henze, D. K. and Seinfeld, J. H.: Global secondary organic aerosol from isoprene oxidation, Geophys. Res. Lett., 33, L09812, doi:10.1029/2006GL025976, 2006.

Kalberer, M., Paulsen, D., Sax, M., Steinbacher, M., Dommen, J., Prevot, A. S. H., Fisseha, R.,

Weingartner, E., Frankevich, V., Zenobi, R., and Baltensperger, U.: Identification of polymers as major components of atmospheric organic aerosols, Science, 303(5664), 1659–1662, 2004.

Kanakidou, M., Seinfeld, J. H., Pandis, S. N., Barnes, I., Dentener, F. J., Facchini, M. C., Van Dingenen, R., Ervens, B., Nenes, A., Nielsen, C. J., Swietlicki, E., Putaud, J. P., Balkanski, Y., Fuzzi, S., Horth, J., Moortgat, G. K., Winterhalter, R., Myhre, C. E. L., Tsigaridis, K., Vignati, E., Stephanou, E. G., and Wilson, J.: Organic aerosol and global climate modelling: a review, Atmos. Chem. Phys., 5, 1053–1123, 2005, http://www.atmos-chem-phys.net/5/1053/2005/.

Kleinman, L. I., Springston, S. R., Daum, P. H., Lee, Y.-N., Nunnermacker, L. J., Senum, G. I., Wang, J., Weinstein-Lloyd, J., Alexander, M. L., Hubbe, J., Ortega, J., Canagaratna, M. R., and Jayne, J.: The time evolution of aerosol composition over the Mexico City plateau, Atmos. Chem. Phys. Discuss., 7, 14 461–14 509, 2007.

Kondo, Y., Miyazaki, Y., Takegawa, N., Miyakawa, T., Weber, R. J., Jimenez, J. L., Zhang, Q., and Worsnop, D. R.: Oxygenated and water-soluble organic aerosols in Tokyo, J. Geophys. Res., 112(D1), 11, doi:10.1029/2006JD007056, 2007.

Loeffler, K. W., Koehler, C. A., Paul, N. M., and De Haan, D. O.: Oligomer formation in evaporating aqueous glyoxal and methyl glyoxal solutions, Environ. Sci. Technol., 40(20), 6318–6323, 2006.

Modey, W. K. and Eatough, D. J.: Twenty four-hour PC-BOSS air-monitoring results from the NETL fine-particulate sampling site in Pittsburgh, Pennsylvania: an annual perspective, Aerosol Sci. Technol., 38(3), 194–204, 2004.

Nenes, A., Pandis, S. N., and Pilinis, C.: ISORROPIA: A new thermodynamic equilibrium model for multiphase multicomponent inorganic aerosols, Aquat. Geochem., 4(1), 123–152, 1998.

Offenberg, J. H., Kleindienst, T. E., Jaoui, M., Lewandowski, M., and Edney, E. O.: Thermal properties of secondary organic aerosols, Geophys. Res. Lett., 33, L03816, doi:10.1029/2005GL024623, 2006.

Orsini, D. A., Ma, Y. L., Sullivan, A., Sierau, B., Baumann, K., and Weber, R. J.: Refinements to the particle-into-liquid sampler (PILS) for ground and airborne measurements of water soluble aerosol composition, Atmos. Environ., 37(9–10), 1243–1259, 2003.

Parrish, D. D., Holloway, J. S., and Fehsenfeld, F. C.: Routine, Continuous Measurement of Carbon Monoxide with Parts per Billion Precision, Environ. Sci. Technol., 28(9), 1615–1618, 1994.

SOA and nitrate volatility in Mexico City

C. J. Hennigan et al.

Title Page

Abstract | Introduction

Conclusions | References

Tables | Figures

◄ | ►

◄ | ►

Back | Close

Full Screen / Esc

Printer-friendly Version

Interactive Discussion

Ryerson, T. B., Williams, E. J., and Fehsenfeld, F. C.: An efficient photolysis system for fast-response NO2 measurements, J. Geophys. Res., 105(D21), 26 447–26 462, doi:10.1029/2000JD900389, 2000.

Sander, S. P., Friedl, R. R., Golden, D. M., Kurylo, M. J., Moortgat, G. K., Keller-Rudek, H., Wine, P. H., Ravishankara, A. R., Kolb, C. E., Molina, M. J., Finlayson-Pitts, B. J., Huie, R. E., and Orkin, V. L.: Chemical kinetics and photochemical data for use in atmospheric studies, Evaluation Number 15, JPL Publication 06-2, Jet Propulsion Laboratory, Pasadena, 2006.

Salcedo, D., Onasch, T. B., Dzepina, K., Canagaratna, M. R., Zhang, Q., Huffman, J. A., De-Carlo, P. F., Jayne, J. T., Mortimer, P., Worsnop, D. R., Kolb, C. E., Johnson, K. S., Zuberi, B., Marr, L. C., Volkamer, R., Molina, L. T., Molina, M. J., Cardenas, B., Bernabe, R. M., Marquez, C., Gaffney, J. S., Marley, N. A., Laskin, A., Shutthanandan, V., Xie, Y., Brune, W., Lesher, R., Shirley, T., and Jimenez, J. L.: Characterization of ambient aerosols in Mexico City during the MCMA-2003 campaign with Aerosol Mass Spectrometry: results from the CENICA Supersite, Atmos. Chem. Phys., 6, 925–946, 2006,
http://www.atmos-chem-phys.net/6/925/2006/.

Seinfeld, J. H. and Pandis, S. N.: Atmospheric Chemistry and Physics, From Air Pollution to Climate Change, John Wiley & Sons, New York, NY, 1998.

Seinfeld, J. H. and Pankow, J. F.: Organic atmospheric particulate material, Annu. Rev. Phys. Chem., 54, 121–140, 2003.

Shaw, W. J., Pekour, M. S., Coulter, R. L., Martin, T. J., and Walters, J. T.: The daytime mixing layer observed by radiosonde, profiler, and lidar during MILAGRO, Atmos. Chem. Phys. Discuss., 7, 15 025–15 065, 2007.

Shetter, R. E. and Muller, M.: Photolysis frequency measurements using actinic flux spectroradiometry during the PEM-Tropics mission: Instrumentation description and some results, J. Geophys. Res., 104(D5), 5647–5662, doi:10.1029/98JD01381, 1999.

Sjostedt, S. J., Huey, L. G., Tanner, D. J., Peischl, J., Chen, G., Dibb, J. E., Lefer, B., Hutterli, M. A., Beyersdorf, A. J., Blake, N. J., Blake, D. R., Sueper, D., Ryerson, T., Burkhart, J., and Stohl, A.: Observations of hydroxyl and the sum of peroxy radical at Summit, Greenland during summer 2003, Atmos. Environ., 41, 5122–5137, 2007.

Stone, E. A., Snyder, D. C., Sheesley, R. J., Sullivan, A. P., Weber, R. J., and Schauer, J. J.: Source apportionment of fine organic aerosol in Mexico City during the MILAGRO Experiment 2006, Atmos. Chem. Phys. Discuss., 7, 9635–9661, 2007,
http://www.atmos-chem-phys-discuss.net/7/9635/2007/.

SOA and nitrate volatility in Mexico City

C. J. Hennigan et al.

Sullivan, A. P., Weber, R. J., Clements, A. L., Turner, J. R., Bae, M. S., and Schauer, J. J.: A method for on-line measurement of water-soluble organic carbon in ambient aerosol particles: Results from an urban site, Geophys. Res. Lett., 31, L13105, doi:10.1029/2004GL019681, 2004.

Sullivan, A. P., Peltier, R. E., Brock, C. A., de Gouw, J. A., Holloway, J. S., Warneke, C., Wollny, A. G., and Weber, R. J.: Airborne measurements of carbonaceous aerosol soluble in water over northeastern United States: Method development and an investigation into water-soluble organic carbon sources, J. Geophys. Res., 111, D23S46, doi:10.1029/2006JD007072, 2006.

Wilson, W. E., Grover, B. D., Long, R. W., Eatough, N. L., and Eatough, D. J.: The measurement of fine particulate semivolatile material in urban aerosols, J. Air Waste Manage. Assoc., 56(4), 384–397, 2006.

Yu, J. Z., Yang, H., Zhang, H. Y., and Lau, A. K. H.: Size distributions of water-soluble organic carbon in ambient aerosols and its size-resolved thermal characteristics, Atmos. Environ., 38(7), 1061–1071, 2004.

SOA and nitrate volatility in Mexico City

C. J. Hennigan et al.

Title Page

Abstract	Introduction
Conclusions	References
Tables	Figures

|◄ | ►|

◄ | ►

Back | Close

Full Screen / Esc
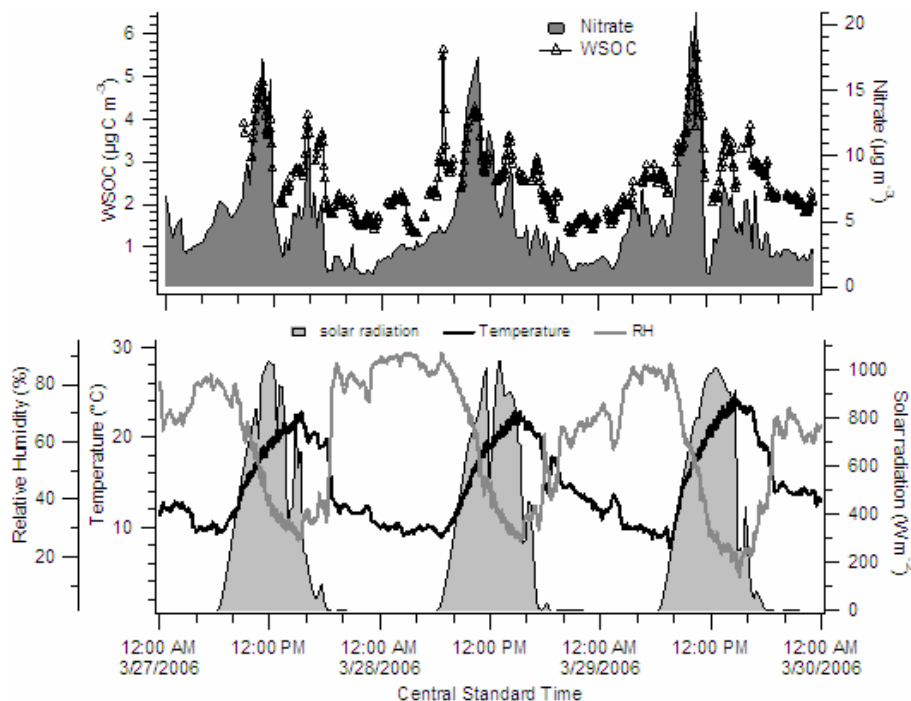
Printer-friendly Version

Interactive Discussion

Fig. 1. Time series of measured NO_3^-, WSOC, solar radiation, temperature, and RH for 27–29 March. Concentrations of NO_3^- and WSOC began to rise shortly after sunrise and model results (not shown) indicate that approximately 75% of the morning concentration increases were due to secondary aerosol formation.

Printer-friendly Version

Interactive Discussion
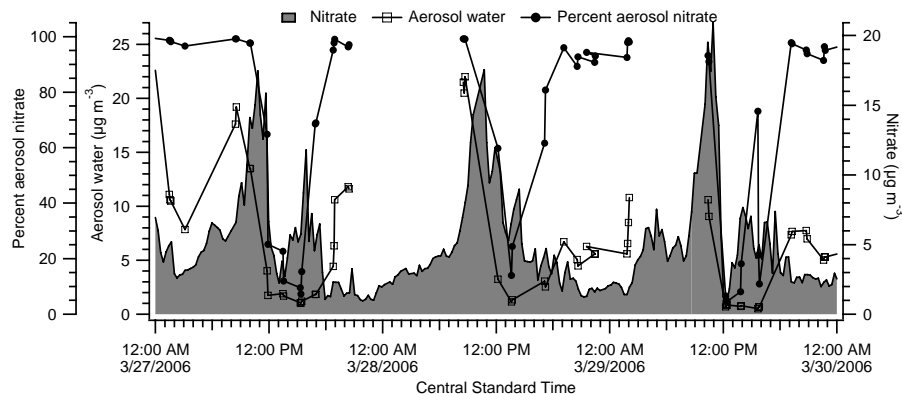
Fig. 2. ISORROPIA-II model output (Percent aerosol nitrate and aerosol water) and measured NO_3^- for 27–29 March. Based on rising morning temperature and decreasing RH, a sharp decrease in the predicted aerosol water concentration was followed by a rapid equilibrium shift in NO_3^- from the aerosol to the gas phase. This equilibrium shift likely produced at least a third of the observed nitrate concentration decrease.
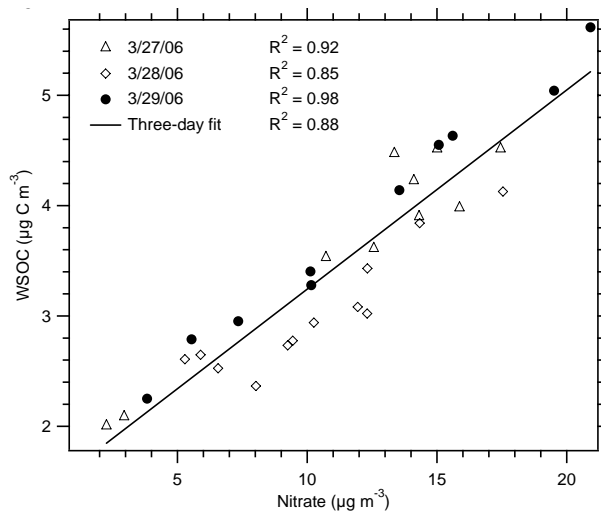
Fig. 3. Correlations between NO_3^- and WSOC during the hours of 08:00–12:45 on the three days of interest. The high correlation indicates similar sources and atmospheric processing of the two species.